Proc. Natl. Acad. Sci. USA
Vol. 82, pp. 4127–4131, June 1985
Cell Biology

Theoretical treatment of microtubules disappearing in solution

(GTP cap/phase change/Monte Carlo method/comparison with experiment)

YI-DER CHEN AND TERRELL L. HILL

Laboratory of Molecular Biology, National Institute of Arthritis, Diabetes, and Digestive and Kidney Diseases, National Institutes of Health, Bethesda, MD 20205

Contributed by Terrell L. Hill, January 15, 1985

ABSTRACT **The origin of the two-phase (cap, no cap) macroscopic kinetic model of the end of a microtubule is reviewed. The model is then applied to a new theoretical problem, namely, the Mitchison–Kirschner [Mitchison, T. & Kirschner, M. W. (1984) *Nature (London)* 312, 237–242] experiment in which aggregated microtubules in solution spontaneously decrease in number (shorten to disappearance) while the surviving microtubules increase in length. The model fits the experiments without difficulty.**

In this paper, the theory of the two-phase model of a microtubule (MT) end is extended to a new experimental problem, but we begin with a review of the origin of the model.

The previous view of MT aggregation, originating with the ideas of Wegner (1) and extended and summarized by Hill and Kirschner (2), was that hydrolysis of GTP-tubulin to GDP-tubulin is closely coupled to the aggregation of GTP-tubulin from solution onto the end of a MT. Thus, a MT would consist entirely of GDP-tubulin units. Treadmilling (1, 2) is an interesting consequence for a free MT in solution. However, this picture was upset by Carlier and Pantaloni (3), who found that the hydrolysis of GTP-tubulin lags behind its aggregation. Hence, there can be a steady-state or transient cap of GTP-tubulin or mostly GTP-tubulin units at each end of a MT, though the interior of a MT is all GDP-tubulin.

When these new kinetic details were incorporated by Hill and Carlier (4) and by Chen and Hill (5) into a theoretical analysis of the steady-state aggregation flux $J_\alpha(c)$ of, say, the α end of a MT, where c is the concentration of free GTP-tubulin, it was found that the theoretical $J_\alpha(c)$ has a discontinuity in slope or a sharp bend at or near the critical concentration $c = c_\alpha$ (where $J_\alpha = 0$). This is a new feature that is a consequence of the GTP cap: the phase or regime above $c = c_\alpha$ is characterized by a significant mean cap of GTP-tubulin whereas the phase or regime below $c = c_\alpha$ has a mean cap whose size decreases rapidly as c is decreased. These theoretical results led Carlier *et al.* (6) to carry out dilution experiments on MTs in solution that confirmed the predicted near-discontinuity in the slope of $J(c)$ at the critical concentration c_∞ (where $J = 0$). Then transient Monte Carlo calculations (6), using the same detailed or "microscopic" kinetic model as above, led to early-time shapes of $J_\alpha(c)$ curves in agreement with the dilution experiments. It was emphasized (6) that the GTP cap stabilizes a MT end and that the absence of a cap leads to instability and fast depolymerization, as exhibited by the relatively steep slope of $J(c)$ below $c = c_\infty$.

The next step, in this alternation between experiment and theory, was the experiments of Mitchison and Kirschner (7, 8) in which MTs formed from centrosomes, axonemes, or seeds were examined visually and individually to achieve a deeper level of detail. These experiments could be interpreted only by adding one further qualitative feature to the conclusions in refs. 4–6: not only were there two different phases (cap, stable; no cap, unstable) above and below $c = c_\alpha$ (for the α end), as described above, but, over a range in c on either side of $c = c_\alpha$, both phases can exist and interconvert (infrequently) at any given c. The capped phase dominates in these interconversions (phase changes) above $c = c_\alpha$ whereas the uncapped phase dominates below $c = c_\alpha$—in agreement with the mean flux $J_\alpha(c)$ results already mentioned. As a consequence of the Mitchison–Kirschner experiments, previous (and new) Monte Carlo steady-state cases were examined (9) at very short time intervals, to look for these alternations in phase. At any c not too far from c_α, such phase changes were indeed found: in the time course of the steady-state Monte Carlo simulation, a MT end switches occasionally and cleanly from one phase to the other (cap or no cap). These Monte Carlo results then made it apparent that the detailed microscopic kinetic scheme (4–6) for each MT end, which formed the basis for the simulation, could be replaced by a much simpler quantitative macroscopic kinetic model (9) based on the existence of the two phases. The two schemes are essentially equivalent and relate to the same system (the end of a MT) but, because of the clean phase changes seen in the simulation, the relatively simple macroscopic model is an excellent approximation to the much more complex microscopic kinetic scheme. The rate constants in the macroscopic model are of course effective composites of microscopic rate constants. Recent theoretical work on this subject (10–12), including comparison with the Mitchison–Kirschner experiments (7, 8), has been based on the new macroscopic kinetic model (9). This program is continued here with the examination of another problem.

The objective here is to apply the two-phase macroscopic kinetic model, for each end of a MT, to the experiment in figure 4 of ref. 8. In this experiment MTs were grown from seeds in a solution with an initially high concentration of free GTP-tubulin. After shearing and then further rapid growth until the amount of tubulin in polymers became essentially constant, samples were taken over the next 55 min, from which were obtained the (decreasing) concentration of surviving MTs, the mean length (which increased) of surviving MTs, and the length distributions of these MTs (not shown in ref. 8 but kindly made available to us by the authors).

The model and basic equations that apply to this problem were introduced in ref. 11. Because the concentration of free GTP-tubulin varies somewhat with time (see below), there is no hope of an analytical solution. Also numerical solution of the set of kinetic master equations (equations 17–21 of ref. 11) is impractical because of the huge number of equations involved. Therefore we have used a Monte Carlo simulation on an initial group of 1550 MTs in a suitable small volume V, treated as a single kinetic system.

The basic kinetic model (9, 10) used for each end is shown in Fig. 1 for the α end. All of these rate constants are func-

The publication costs of this article were defrayed in part by page charge payment. This article must therefore be hereby marked "*advertisement*" in accordance with 18 U.S.C. §1734 solely to indicate this fact.

Abbreviation: MT, microtubule.

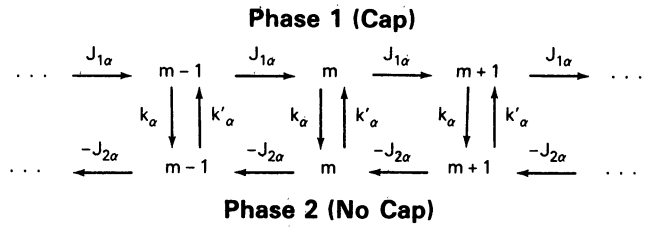

FIG. 1. Two-phase macroscopic kinetic model or diagram for the α end of a MT.

tions of c (see below), the concentration of free GTP-tubulin. The variable m in this figure counts subunits added to or lost from the α end. For a complete polymer, with two ends, the corresponding kinetic diagram (11) is given in Fig. 2. The J_{ij} shown in Fig. 2*a* are composites of J_1 and J_2 (Fig. 1) for the α and β ends (11):

$$J_{11} \equiv J_{1\alpha} + J_{1\beta}, \quad J_{12} \equiv -J_{1\alpha} - J_{2\beta}$$
$$J_{21} \equiv -J_{2\alpha} - J_{1\beta}, \quad J_{22} \equiv -J_{2\alpha} - J_{2\beta}. \qquad [1]$$

The subscripts i and j on J_{ij} ($i, j = 1, 2$) refer to the phases of ends α and β, respectively. In cases of interest, all of the J_{ij} are positive. The polymer lengthens in state 11 and shortens in states 12, 21, and 22 (i.e., if one or both ends have no GTP cap). The transition from $m = 1$ in state 22 (both ends shortening) is assumed to lead to polymer disappearance. The transitions from $m = 1$ in states 12 and 21 correspond to the loss of the last subunit from the shortening end. This leaves a polymer (state 0) that consists only of the cap that was at the other end. This residual cap is essentially a seed that can now start to grow from either end (J_{11} transition out of state 0). Alternatively, the residual cap may be too small to be stable, in which case it would disintegrate (γ transition out of state 0). Homogeneous nucleation of new polymers is assumed not to occur. Thus m in Fig. 2*a* refers to the number of subunits in the polymer in addition to the number in the residual cap, which we call m_c (a constant). In the γ transition, m_c subunits become free in solution. In the last J_{22} transition, $m_c + 1$ subunits become free.

The phase change rate constants shown in Fig. 2*b* apply to every $m \geq 1$. The values of m usually populated are in the hundreds and thousands. Hence possible m dependence of rate constants at very small m are ignored. However, all rate constants are functions of c.

In the Monte Carlo simulation, each of the surviving MTs does a random walk on its own kinetic diagram (Fig. 2). However, the whole collection of surviving MTs in V must be treated as a single system because gain or loss of polymer subunits in the J_{ij} or γ transitions alters the concentration of free subunits (GTP-tubulin), which in turn alters the rate constants. The volume V of the solution is constant, as is the total number of subunits (free or in polymers).

We turn now to the actual rate constants used. Analytical expressions are needed for each of these. Mitchison and Kirchner (7) found $c_\infty = 14$ μM (critical concentration) but the true $c_\infty \cong 10$ μM, because of inactive tubulin. Therefore we correct the constants 3.82 and 1.22 in table 1 of ref. 8 by a factor 14/10 to obtain

$$J_{1\alpha} = 5.35c - 0.37, \quad J_{1\beta} = 1.71c - 1.1. \qquad [2]$$

The units throughout the paper are s^{-1} for all first-order rate constants and μM for c. At $c = 0$ (8), $J_{2\alpha} = -340$ and $J_{2\beta} = -212$, but there is no experimental information about the c dependence of these two quantities. We therefore use the shape of curve found in the five-helix Monte Carlo work (12) but reduce the amplitude of the c dependence to keep all J_{ij} positive at $c = 20$ (needed below). We use the empirical formulas

$$J_{2\alpha} = -378.7 + 138.1[a/(1 + a)]$$
$$J_{2\beta} = -236.1 + 86.1[a/(1 + a)] \qquad [3]$$
$$a = \exp[(c - 3)/3.18].$$

The four functions in Eqs. 2 and 3 are included in Fig. 3.

We again have to resort to five-helix Monte Carlo results (12) for the ks. For lack of other information, we assume both ends have the same k and k'. Empirical equations fitting the Monte Carlo simulations (12) are as follows:

$$k_\alpha = k_\beta = k = 0.841/c^{2.474},$$
$$k'_\alpha = k'_\beta = k' = 1.6 \times 10^{-5}c^3. \qquad [4]$$

The k and k' functions in Fig. 4 are both smaller than those in Eqs. 4 by a constant factor of 2.5 (as explained below).

Very long (i.e., nondisappearing) polymers with the above rate constants (Eqs. 2–4) have the steady-state subunit flux $J(c)$ included in Fig. 3, as calculated from equation 5 of ref. 11. The critical concentration c_∞, where $J = 0$, is $c_\infty = 10.08$ (consistent with ref. 7). The curve $f_1(c)$ at the bottom of the figure is $k'/(k + k')$, the steady-state fraction of ends in state

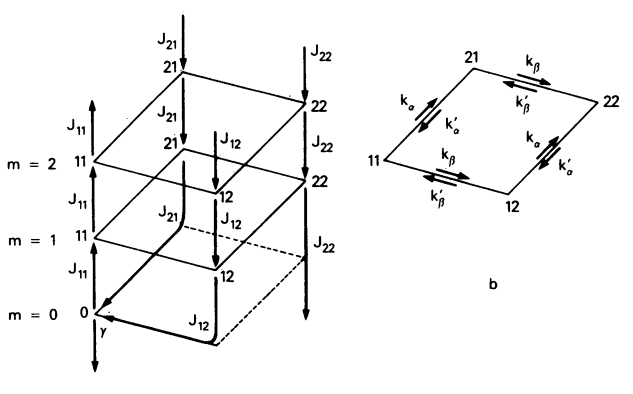

FIG. 2. (*a*) Two-phase kinetic diagram for a MT in solution with two free ends, α and β. J_{ij} and γ are defined in the text. (*b*) Phase change rate constants for every $m \geq 1$.

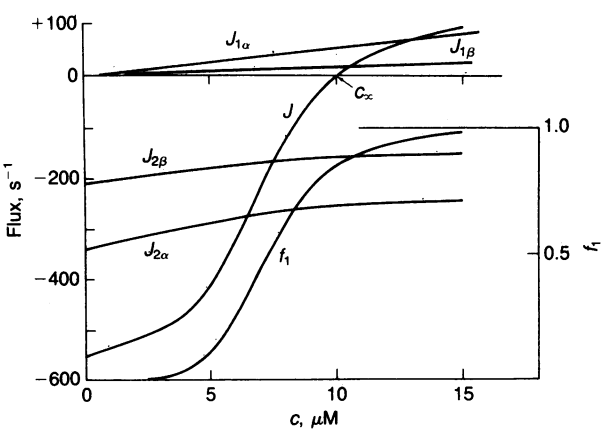

FIG. 3. Steady-state subunit fluxes for α and β ends in phase 1 (cap) and 2 (no cap). J is the overall steady-state subunit flux (both ends) for very long MTs. The fraction of ends in state 1 (cap), at steady state, is f_1.

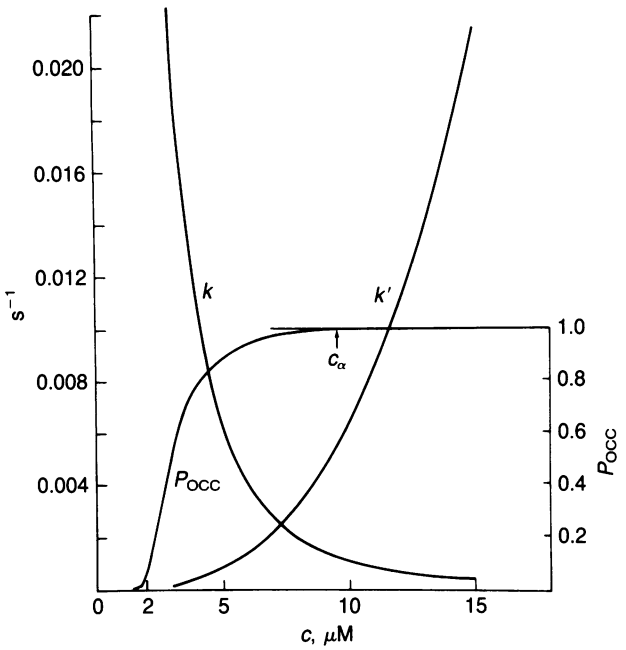

FIG. 4. Phase change rate constants (both ends) used in one example (Eq. 6). Also included is the curve $P_{OCC}(c)$ for the α end based on Eqs. 2, 3, and 6 and on equation 11 of ref. 12.

1 (i.e., with a cap). Other properties at $c = c_\infty$, from Eqs. 2–4, are

$$J_{1\alpha} = 53.6, \quad J_{1\beta} = 16.1, \quad J_{2\alpha} = -254.1, \quad J_{2\beta} = -158.4$$
$$J_{11} = 69.7, \quad J_{12} = 104.8, \quad J_{21} = 237.9, \quad J_{22} = 412.4$$
$$J_\alpha = 9.09, \quad J_\beta = -9.09 \quad (c_\alpha = 9.75, \quad c_\beta = 10.87) \quad [5]$$
$$k = 0.00277, \quad k' = 0.0164, \quad f_1 = 0.8554.$$

Here J_α and J_β are the steady-state fluxes at the two ends (note that there is treadmilling), and c_α and c_β are the critical concentrations of the separate ends (where $J_\alpha = 0$ or $J_\beta = 0$).

The J_{ij} are of order 10^2 s^{-1} while k and k' are of order 10^{-2} s^{-1}, with a ratio of order 10^4. Thus each J_{ij} transition in Fig. 2*a* is more probable than a phase change by a factor of order 10^4. Because of this, only a very small error (which we have examined) is made if the J_{ij} transitions are assumed to occur in packages of g transitions, where we usually take $g = 100$. Using these g packages, the effective rate constants in the resulting modified diagram are J_{ij}/g and γ/g (with no change in k and k'). Without this compression, the cost of a Monte Carlo simulation would be prohibitive because of the very large number of transitions. In two quite different cases, mentioned below, a simulation with $g = 100$ was repeated using $g = 50$; in both cases, as expected, the change in g had no noticeable effect on the results.

Another somewhat similar simplification was introduced to reduce the cost of the computation. The number of free subunits in the small volume V used in the simulation is more than 10^7. Corrections to the free concentration c were made only after each net gain or loss of 10^4 free subunits (i.e., a change in c of less than 0.1%).

The program (with Eqs. 2–4) was tested first on the 5-min period of very rapid polymer growth after shear (figure 4 of ref. 8), starting with $c = 20$ and an approximately equal number of subunits in the form of polymers. Details are omitted because no information was available on the initial length distribution and hence a guess was made that all initial polymers were in state 11, with a flat distribution in length of reasonable width about the mean length. The value of c decreased to $c_\infty = 10.08$ in 4.25 min and then began to oscillate slightly just below c_∞. After 5 min, polymers were in approximately the c_∞ steady-state distribution among state 11, 12, 21, and 22—i.e., in relative amounts f_1^2, $f_1(1 - f_1)$, etc., with $f_1 = 0.8554$ (Eq. 5). The length distribution was similar in all four states. One of the $g = 50$ versus $g = 100$ tests (see above) was made on this period of rapid growth.

The main Monte Carlo calculations begin (we call this $t = 0$) *after* the above 5-min period of rapid growth. We use the experimental (8) starting ($t = 0$) distribution in length (Fig. 5*A*), smoothed out above 18 μm. The connection adopted between subunit number and length is 5000 subunits = 3 μm. In view of our results in the rapid growth period (above), we assume that $c = c_\infty = 10.08$ at $t = 0$ and that there is a steady-state distribution among states 11, 12, 21, and 22, all with length distribution of the same shape (Fig. 5*A*). We start, for convenience, with 1550 polymers. The initial polymer concentration (figure 4 of ref. 8) is 6.84×10^{11} ml^{-1}. Hence $V = 2.26 \times 10^{-9}$ ml. The initial number of subunits in polymers (Fig. 5*A*) is 3.74×10^7; the initial number of free subunits is 1.37×10^7. The total number of subunits is held fixed.

The initial parameters chosen were Eqs. 2–4, $g = 100$, $m_c = 30$, and $\gamma = 10^4$. Because J_{11} is about 70 (see Eqs. 5), this γ implies that almost every residual cap disintegrates. This case gave somewhat too slow of a decrease in MT number and too slow an increase in mean MT size. However, merely by dividing both k and k' by 2.5—i.e., on using

$$k = 0.3364/c^{2.474}, \quad k' = 6.4 \times 10^{-6}c^3, \quad [6]$$

good agreement was obtained with the experimental results (Fig. 6). The functions in Eqs. 6 are those shown in Fig. 4. This change in k and k' does not affect $J(c)$, c_∞, and $f_1(c)$ in Fig. 3; also, Eqs. 5 are unaltered except for the k and k' values.

In the Eqs. 6 case, almost 2×10^6 transitions (g packages, k, k') were needed to reach $t = 55$ min. At that time 337 polymers remained, distributed as 237 (state 11), 49 (state 12), 41 (state 21), and 10 (state 22). The final $c = 10.11$. The c_∞ steady-state distribution of 337 polymers would be 246, 42, 42, 7. The initial steady-state distribution is soon distorted because state 21 polymers disappear faster than state 12 polymers (see Eqs. 5). But the steady-state distribution is approached again as the surviving polymers become longer. During the simulation c dips below c_∞ (minimum $c = 8.59$ at 3.0 min) and performs damped oscillations primarily just below c_∞. This type of behavior was observed in every simulation. Correspondingly, the number of subunits in polymers is not quite constant with time. The values every 6 min are shown in Table 1.

The same case (Eqs. 6) was run with $g = 50$; no effect other than apparently normal fluctuations was noted. Almost 4×10^6 transitions were required. The combined length distributions for these two cases ($g = 100$, $g = 50$), suitably renormalized, at $t = 5$, 15, 25, 40, and 55 min are compared with experiment (8) in Fig. 5. The agreement appears to be within normal fluctuations. The experimental numbers of polymers in a sample range between 525 and 560; the Monte Carlo numbers of surviving polymers are 2228, 1399, 1071, 791, and 669, at the respective times. Of course the separate Monte Carlo 11, 12, 21, and 22 length distributions are also available, but there are no experiments for comparison.

It should be emphasized that the adjustment to k, k' (Eq. 6) was made solely to fit Fig. 6. The agreement between theory and experiment in Fig. 5 then followed automatically with no further adjustment of rate constants.

The above case (Eq. 6) is by no means unique, although it represents the simplest alteration of the original information that produces agreement with experiment. Two other cases that agree with experiment (Figs. 5 and 6) essentially as well

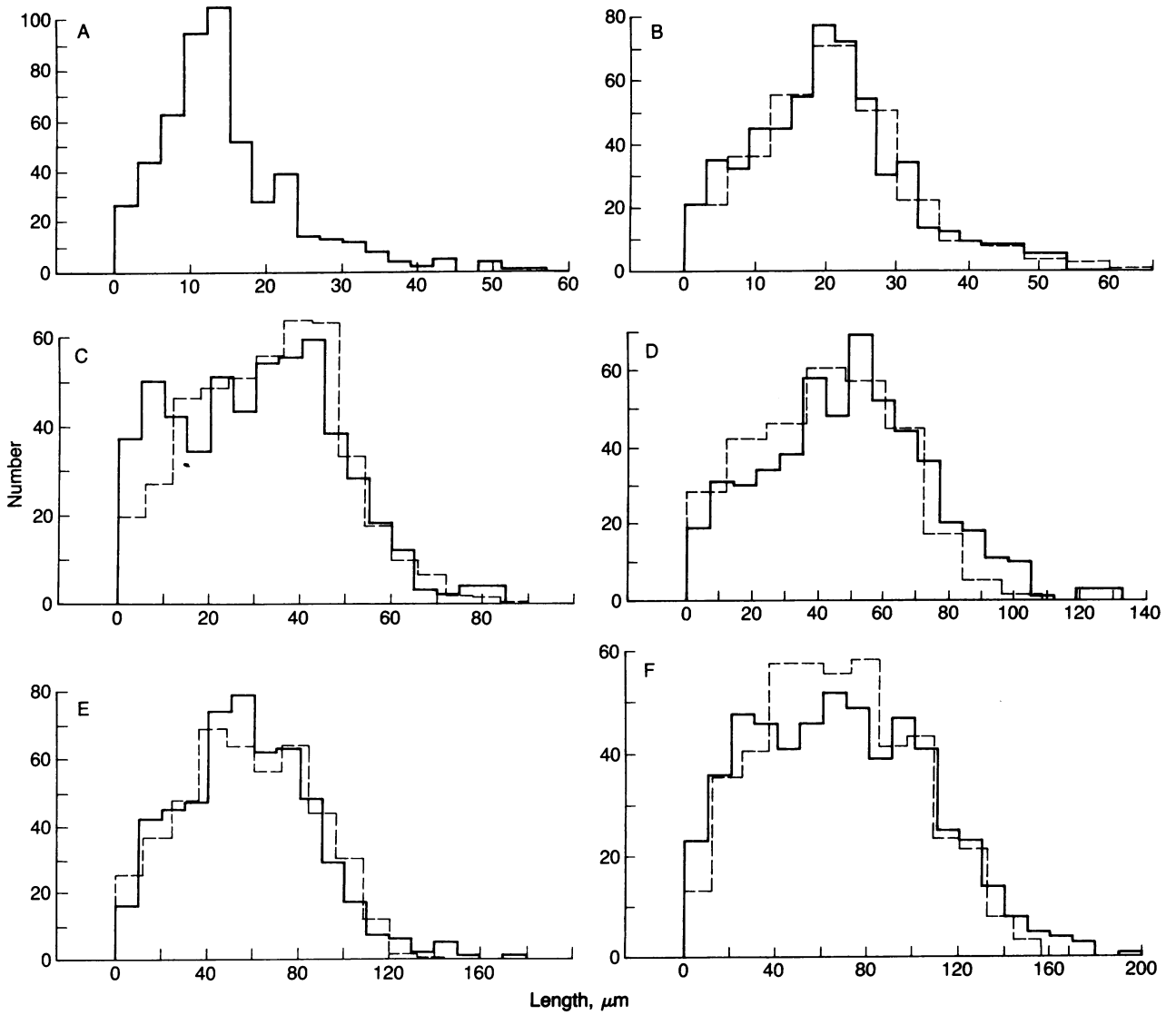

FIG. 5. Solid lines: experimental length distributions at $t = 0$ (*A*), $t = 5$ min (*B*), $t = 15$ min (*C*), $t = 25$ min (*D*), $t = 40$ min (*E*), and $t = 55$ min (*F*). Dashed lines: normalized Monte Carlo length distributions for the Eq. **6** case.

were found easily. In the first case k and k' in Eq. **4** are divided by the constant 5.0 and, in addition, γ is reduced from 10^4 to 60 (the probability that a residual cap disintegrates, at $c = c_\infty$, is then $60/129.7 = 0.46$, from Eqs. **5**). A much smaller γ, e.g., $\gamma = 10$, leads to unsatisfactory bimodal length distributions because of the many new additions to state 11 at small m. For the second case, we start with

$$\gamma = 10^4, \quad J_{2\alpha} = -340 = \text{constant}, \quad J_{2\beta} = -212 = \text{constant}$$
$$k = 0.6285/c^{2.474}, \qquad [7]$$

leaving k' as in Eq. **4**. The coefficient in $k(c)$ was adjusted to give $c_\infty = 10.08$. In this case $f_1(c)$ and $J(c)$ are changed somewhat (results not shown). As with Eqs. **2–4**, the decrease in MT number and the increase in MT size are found to be too slow. However, this is easily corrected by dividing k and k' by the constant 1.725 to yield

$$k = 0.3643/c^{2.474}, \qquad k' = 9.275 \times 10^{-6}c^3. \qquad [8]$$

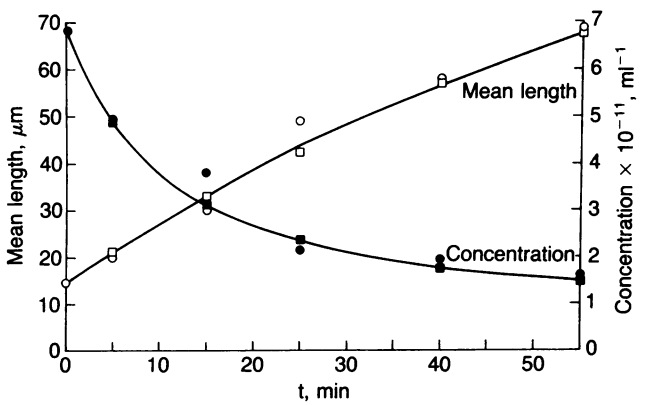

FIG. 6. Comparison of Mitchison–Kirschner experimental points (○, ●) with Monte Carlo points (□, ■) in the Eq. **6** case. The curves are for the Monte Carlo data. ○ and □, mean length; ● and ■, concentration.

Table 1. Number of subunits in polymers (Eq. **6**)

t, min	No. $\times 10^{-7}$	t, min	No. $\times 10^{-7}$	t, min	No. $\times 10^{-7}$
0	3.742	18	3.802	42	3.796
3	3.945	24	3.816	48	3.760
6	3.872	30	3.755	54	3.762
12	3.828	36	3.751		

The value of c_∞ is still 10.08. This last case, with $J_{2\alpha}$ and $J_{2\beta}$ constant (Eqs. 7), is a limiting, actually unrealistic, example. It is not possible for $J_{2\alpha}$ and $J_{2\beta}$ to be strictly constant for this would mean that a MT without a cap (state 2) could never form a cap. A small amount of exchange of GTP for GDP at the MT end, or of attachment of GTP-tubulin to GDP-tubulin at the MT end, would allow a cap to form (12) and would alter $J_{2\alpha}$ and $J_{2\beta}$, as for example in Fig. 3.

In summary, the two-phase macroscopic kinetic model seems able to account very well for the experiments summarized in figure 4 of ref. 8.

As an appendix, the curve $P_{occ}(c)$ was calculated, using the rate constants for the α end in Eqs. **2**, **3**, and **6**, and is included in Fig. 4. P_{occ} is the probability at steady state that a nucleated site on a centrosome will be occupied by an observable MT (of more than 500 subunits). The calculation was made using equation 11 of ref. 12. The corresponding experimental curve is figure 4 of ref. 7. The theoretical curve (Fig. 4) starts up at the same c as the experimental curve (corrected for inactive tubulin) but the theoretical curve rises faster. In particular, P_{occ} (theoretical) = 1 at the critical concentration c_α = 9.75 μM. The discrepancy is to be expected because the theoretical curve refers to steady state but the experiments never reached steady state.

We are indebted to Tim Mitchison and Marc Kirschner for providing the MT length distributions from the experiment in figure 4 of ref. 8.

1. Wegner, A. (1976) *J. Mol. Biol.* **108**, 139–150.
2. Hill, T. L. & Kirschner, M. W. (1982) *Int. Rev. Cytol.* **78**, 1–125.
3. Carlier, M.-F. & Pantaloni, D. (1981) *Biochemistry* **20**, 1918–1924.
4. Hill, T. L. & Carlier, M.-F. (1983) *Proc. Natl. Acad. Sci. USA* **80**, 7234–7238.
5. Chen, Y. & Hill, T. L. (1983) *Proc. Natl. Acad. Sci. USA* **80**, 7520–7523.
6. Carlier, M.-F., Hill, T. L. & Chen, Y. (1984) *Proc. Natl. Acad. Sci. USA* **81**, 771–775.
7. Mitchison, T. & Kirschner, M. W. (1984) *Nature (London)* **312**, 232–237.
8. Mitchison, T. & Kirschner, M. W. (1984) *Nature (London)* **312**, 237–242.
9. Hill, T. L. & Chen, Y. (1984) *Proc. Natl. Acad. Sci. USA* **81**, 5772–5776.
10. Hill, T. L. (1984) *Proc. Natl. Acad. Sci. USA* **81**, 6728–6732.
11. Hill, T. L. (1985) *Proc. Natl. Acad. Sci. USA* **82**, 431–435.
12. Chen, Y. & Hill, T. L. (1985) *Proc. Natl. Acad. Sci. USA* **82**, 1131–1135.